AWARD NUMBER: W81XWH-15-1-0729

TITLE: MYC RNAi-PT Combination Nanotherapy for Metastatic Prostate Cancer Treatment

PRINCIPAL INVESTIGATOR: Angelo M. De Marzo

CONTRACTING ORGANIZATION: The Johns Hopkins University
Baltimore, MD 21250

REPORT DATE: October 2016

TYPE OF REPORT: Annual

PREPARED FOR: U.S. Army Medical Research and Materiel Command
Fort Detrick, Maryland 21702-5012

REPORT DOCUMENTATION PAGE

Form Approved
OMB No. 0704-0188

1. REPORT DATE	2. REPORT TYPE	3. DATES COVERED
October 2016	Annual	30 Sep 2015 – 29 Sep 2016

4. TITLE AND SUBTITLE

MYC RNAi-PT Combination Nanotherapy for Metastatic Prostate Cancer Treatment

5a. CONTRACT NUMBER

5b. GRANT NUMBER
W81XWH-15-1-0729

5c. PROGRAM ELEMENT NUMBER

6. AUTHOR(S)
Omid Farokhzad (initiating PI), Angelo De Marzo (partnering PI), Charles Bieberich (partnering PI), Srinivasan Yegnasubramanian (co-I), Jinjun Shi (co-I)

E-Mail: ofarokhzad@bwh.harvard.edu

5d. PROJECT NUMBER

5e. TASK NUMBER

5f. WORK UNIT NUMBER

7. PERFORMING ORGANIZATION NAME(S) AND ADDRESS(ES)

Brigham and Women's Hospital, Boston, MA 02115

University of Maryland, Baltimore County, Baltimore, MD 21250

The Johns Hopkins University School of Medicine, Baltimore, MD 21205

8. PERFORMING ORGANIZATION REPORT NUMBER

9. SPONSORING / MONITORING AGENCY NAME(S) AND ADDRESS(ES)

U.S. Army Medical Research and Materiel Command
Fort Detrick, Maryland 21702-5012

10. SPONSOR/MONITOR'S ACRONYM(S)

11. SPONSOR/MONITOR'S REPORT NUMBER(S)

12. DISTRIBUTION / AVAILABILITY STATEMENT

Approved for Public Release; Distribution Unlimited

13. SUPPLEMENTARY NOTES

14. ABSTRACT

The main objective of this project is to develop an innovative nanotherapy modality by combining platinum (Pt) chemotherapy and MYC-targeting RNA interference (RNAi) for more effective treatment of metastatic prostate cancer (PCa). In Year 1 of this project, we have made substantial progress and accomplishments under the proposed tasks. We synthesized, characterized and screened a large library of lipid-polymer hybrid NPs for siRNA delivery, by systematically exploring (i) the effect of organic solvent on the NP formulation; (ii) the effect of surface lipid-PEG on NP behaviors in vitro and in vivo; and (iii) the use of redox-sensitive polymers for triggered siRNA release and enhanced gene silencing. The optimized siRNA NPs showed effective MYC silencing in vitro, as demonstrated by the western blot and immuno-fluorescence results. We also synthesized a series of cisplatin prodrugs as planned for NP encapsulation and in vitro cytotoxicity test. In parallel, we have established cell lines derived from sites of metastasis of MYC-driven transgenic BMPC tumors and performed MYC signature analysis in BMPC mice by RNAseq. We further demonstrate MYC silencing in BMPC cell line-based allograft tumors by the hybrid NPs.

15. SUBJECT TERMS
Nanotechnology, nanoparticle, siRNA delivery, platinum, MYC, prostate cancer, drug resistance, mouse model, pathology, genomics

16. SECURITY CLASSIFICATION OF:			17. LIMITATION OF ABSTRACT	18. NUMBER OF PAGES	19a. NAME OF RESPONSIBLE PERSON
a. REPORT	b. ABSTRACT	c. THIS PAGE			USAMRMC
Unclassified	Unclassified	Unclassified	Unclassified	27	19b. TELEPHONE NUMBER *(include area code)*

Table of Contents

Page

1. INTRODUCTION

The main objective of this project is to develop an innovative nanotherapy modality by combining platinum (Pt) chemotherapy and MYC-targeting RNA interference (RNAi) for more effective treatment of metastatic prostate cancer (PCa). Two specific aims are proposed in this study, including (i) development and optimization of MYC siRNA-Pt nanoparticles (NPs), and (2) determination of the efficacy of select NPs in the $B13^{MYC/Cre}|Pten^{fl/fl}$ engineered PCa mouse model. This project is directed by an interdisciplinary team in the PCa research field, including Initiating PI Dr. Omid Farokhzad from Brigham and Women's Hospital (BWH)/Harvard Medical School (HMS), Partnering PIs Dr. Charles Bieberich from the University of Maryland Baltimore County (UMBC) and Dr. Angelo De Marzo from the John Hopkins University (JHU), and two co-investigators (Dr. Srinivasan Yegnasubramanian from JHU and Dr. Jinjun Shi from BWH/HMS).

2. KEYWORDS

Nanotechnology, lipid, polymer, hybrid nanoparticle, siRNA delivery, platinum, MYC, prostate cancer, drug resistance, mouse model, pathology, genomics

3. ACCOMPLISHMENTS

- **What were the major goals of the project?**

The project has two specific aims. The major tasks and subtasks in the SOW are shown below.

Specific Aim 1: Development and optimization of MYC siRNA-Pt NPs
Major Task 1. Rational design and creation of siRNA-Pt NPs: (i) NP optimization for effective gene silencing; (ii) Synthesis of cisplatin prodrugs; and (iii) siRNA-Pt NP development
Major Task 2. In vitro evaluation and mechanism studies: (i) Cellular cytotoxicity of MYC siRNA-Pt NPs; and (ii) Mechanism study of the MYC role in Pt resistance
Major Task 3. In vivo test and optimization: (i) In vivo studies of select hybrid NPs; and (ii) In vivo evaluation of siRNA-Pt NPs

Specific Aim 2: Determination of the efficacy of select RNAi-Pt NPs in the $B13^{MYC/Cre}|Pten^{fl/fl}$ engineered PCa mouse model
Major Task 4. Evaluation of MYC silencing in this genetically engineered mouse model: (i) NP BioD and MYC silencing; and (ii) Assessment of a MYC gene expression signature to track pharmacodynamic response of MYC siRNA-Pt NP therapy
Major Task 5. Investigation of tumor development/progression to metastasis and side effects after NP administration: (i) Effect of MYC siRNA-Pt NPs on PCa progression to metastasis; (ii) Effect of siRNA-Pt NPs on survival in $B13^{MYC/Cre}|Pten^{fl/fl}$ males with late stage disease; and (iii) Side effects of the combination nanotherapy

- **What was accomplished under these goals?**

In Year 1 of this project (9/2015 - 9/2016), our efforts are mainly focused on Specific Aim 1. We have made substantial progress and accomplishments for the proposed tasks. We synthesized, characterized and screened a large library of lipid-polymer hybrid NPs for siRNA delivery, by systematically exploring (i) the effect of organic solvent on the NP formulation; (ii) the effect of surface lipid-PEG on NP behaviors in vitro and in vivo; and (iii) the use of redox-sensitive polymers for triggered siRNA release and enhanced gene silencing. The optimized siRNA NPs showed effective MYC silencing in vitro, as demonstrated by the western blot and immuno-fluorescence results. We also synthesized a series of cisplatin prodrugs as planned for NP encapsulation and in vitro cytotoxicity test. In parallel, we have established cell lines derived from sites of metastasis of MYC-driven transgenic BMPC tumors and performed MYC signature analysis in BMPC mice by RNAseq. We further demonstrate MYC silencing in BMPC cell line-based allograft tumors by the hybrid NPs. Below are the accomplishments for each subtask.

Major Task 1. Rational design and creation of siRNA-Pt NPs
(i) NP optimization for effective gene silencing (Farokhzad and Shi, BWH)
In this subtask, we have synthesized and characterized a series of lipid-polymer hybrid NPs for understanding and optimizing this unique siRNA delivery platform (Figure 1a). In the first set of experiments, we investigated the effect of water-miscible organic solvents on the siRNA NP self-assembly, including dimethylformamide (DMF), dimethylsulfoxide (DMSO), acetone, and tetrahydrofuran (THF). Figure 1b shows that sub-100 nm NPs were obtained with DMF and DMSO, which possess relatively high dielectric constants, while larger NPs were formed when using solvents with lower dielectric constants (i.e., acetone and THF). Low dielectric constant of

a solvent implies its low polarity and poor water miscibility. Therefore, when a low dielectric constant solvent is used, the organic solution of PLGA/nanocomplexes would have less efficient dispersion in the lipid-PEG aqueous solution, leading to the formation of larger NPs. DMF was chosen for NP formulation, as the resulting smaller NPs could facilitate better tumor accumulation via the enhanced permeability and retention (EPR) effect. The hybrid siRNA NPs prepared with DMF also exhibited a spherical structure with a narrow size distribution as observed by TEM (Figure 1c).

Next, we conducted a systematic study to explore the effect of surface lipid-PEG on siRNA NP delivery. We found that the lipid-PEG molecules can dissociate from the hybrid NPs in the presence of serum albumin (Figure 1a), which is the most abundant

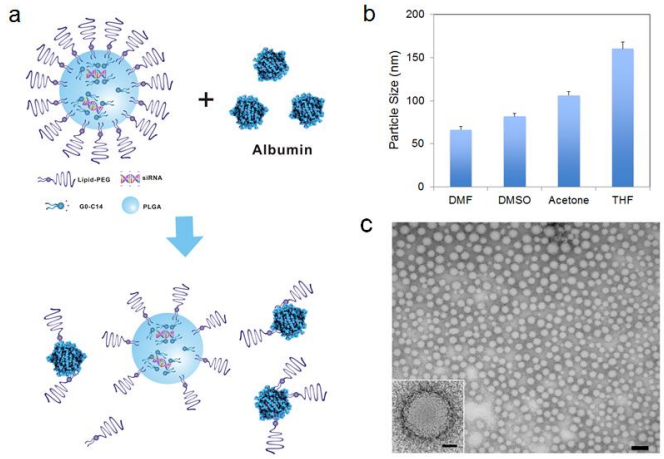

Figure 1. Lipid-polymer hybrid siRNA NPs. (a) Schematic of the NP structure and the lipid-PEG dissociation in the presence of albumin. (b) Size of the hybrid NPs prepared using different organic solvents. (c) TEM image of the NPs prepared with DMF (scale bar: 100nm). The scale bar is 20nm for the insert image.

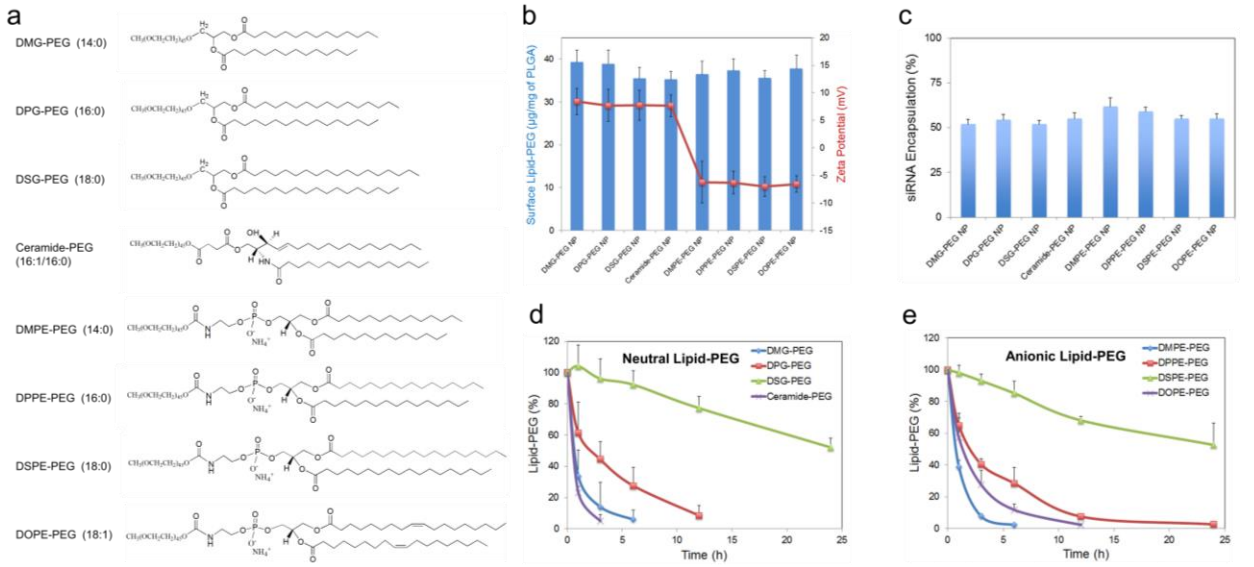

Figure 2. Effect of lipid-PEG on the properties and de-PEGylation of the hybrid siRNA NPs. (a) Chemical structure of eight different lipid-PEGs. (b) The amount of surface lipid-PEG relative to the PLGA polymer weight and the surface charge (zeta potential) on different NPs. (c) siRNA encapsulation efficiency of the NPs with different lipid-PEGs. Dissociation kinetics of (d) neutral lipid-PEGs and (e) anionic lipid-PEGs from respective NPs in the presence of serum albumin.

plasma protein and can bind avidly to diacyl lipids. We hypothesized that both the assembly and the dissociation processes might be predominantly determined by the physicochemical properties of the lipid-PEG molecules. In this experiment, a series of 8 lipid-PEGs with different alkyl chains and charges (Figure 2a) were used to evaluate their effect on the behaviors of the hybrid NPs for siRNA delivery, while keeping the PEG molecular weight (2 kDa) consistent. They are divided into two categories, neutral and anionic lipid-PEGs, based on the linkage (glycerol/serine vs. glycero-3-phosphoethanolamine) between the lipophilic tails and the PEG chain. Both

categories include three lipid-PEGs with saturated alkyl chains of different length (C14, C16 and C18) and one lipid-PEG with unsaturated chain(s) (ceramide or DOPE).

We first quantified the amount of lipid-PEG that self-assembled on the NPs using a reported method based on the spectrophotometric measurement of complexes formed by PEG and barium iodide. All NPs carried a similar amount of lipid-PEGs on the surface, which was ~ 35-40 μg/mg of the PLGA polymer (Figure 2b). The hybrid NPs prepared with neutral vs. anionic lipid-PEGs also carried different surface charges (Figure 2b). The NPs coated with neutral lipid-PEGs showed mildly positive zeta potential (~ 8 mV), while those with anionic lipid-PEGs exhibited mildly negative charges (~ -7 mV). The choice of lipid-PEGs also had no significant influence on the particle size (~ 60-70 nm) and the encapsulation efficiency of siRNA, which was ~ 50-60% for all the NPs (Figure 2c) as measured using fluorophore labeled siRNA (DY547-siRNA).

We then investigated the dissociation kinetics of lipid-PEGs from respective hybrid siRNA NPs in 4 % (w/v) serum albumin in phosphate buffered saline (PBS) as simulated plasma, considering that albumin is the main plasma protein in blood and has a strong binding with diacyl lipids. While all lipid-PEGs dissociated from NPs over time as shown in Figure 2d-e, the rate of dissociation was drastically different. For lipid-PEGs with saturated tails in both neutral and anionic categories, shorter alkyl chains resulted in faster dissociation. For example, after 24 h incubation with albumin, over 50% of DSG-PEG and DSPE-PEG (with C18 alkyl chains) were still remained on NP surfaces. As a comparison, the amount of DMG-PEG and DMPE-PEG (with C14 alkyl chains) dwindled below the detection limit after 6-12 h. This phenomenon might be explained by the higher phase transition temperature and lower fluidity of the lipid tails with longer saturated alkyl chains, which could result in stronger hydrophobic interactions with the PLGA core. Interestingly, much faster dissociation was observed for the unsaturated lipid-PEGs than the saturated ones with the same length of alkyl chain (ceramide vs. DPG, or DOPE vs. DSPE). DOPE-PEG, which carries two unsaturated C18 alkyl chains, was released at a r ate even faster than DPPE-PEG with two saturated C16 alkyl chains. Similarly, ceramide-PEG (with one unsaturated C16) was released faster than DMG-PEG (saturated C14). This may be attributed to the fact that the unsaturation on alkyl chain can lower the chain melting transition temperature, and thus increase the lipid fluidity. On the other hand, neutral and anionic lipid-PEGs with the same alkyl chains showed similar dissociation kinetics, suggesting that the charge in the linkage group between PEG and alkyl chains had negligible effect on the de-PEGylation of these NPs.

In addition, we have designed and developed redox-responsive polymers to replace the PLGA polymer in the NP's core. Whereas this study was not in the original research plan, we think it could further improve siRNA delivery to cancer cells. As one of the unique hallmarks of cancer, the intra-cellular levels of glutathione (GSH) are ~100-1000 fold higher in cancer cells than in normal tissue, thus providing a fascinating natural stimulus for triggered cytosolic drug/gene delivery. Moreover, elevated GSH levels have been correlated with the progression and drug resistance

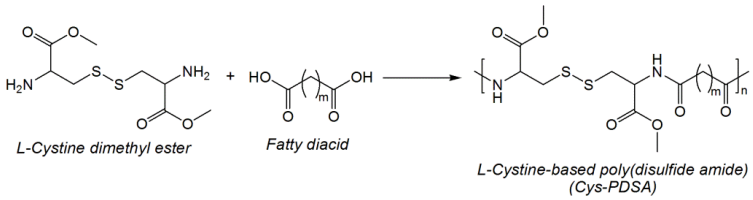

	Poly(disulfide amide)	M_n	M_w	Polydispersity
m = 4	Cys-PDSA4	2900	4300	1.48
m = 6	Cys-PDSA6	3900	5700	1.46
m = 8	Cys-PDSA8-1	4700	7800	1.66
m = 8	Cys-PDSA8-2	5700	7300	1.43
m = 8	Cys-PDSA8-3	9300	15200	1.63
m = 8	Cys-PDSA8-4	11700	16600	1.42

Figure 3. Synthesis route and feed compositions of the redox-responsive Cys-PDSA polymers.

development of different cancers including aggressive PCa. The redox-responsive polymers were synthesized via the condensation polymerization between L-cystine ester and aliphatic dicarboxylic acids (Figure 3). The L-cystine ester provides redox-responsive property due to the presence of disulfide bond in its structure. By condensation with fatty diacids with varied aliphatic chain length, the Cys-PDSA polymer can be finely tuned for rationally designing hydrophobicity and redox response of the resulting hybrid NPs. We synthesized six polymers with different molecular weights and investigated their redox response. Figure 4 shows the NMR spectrum and GPC profile of one representative polymer, Cys-PDSA8-2. The typical signals corresponding to the protons of L-cystine ester and fatty diacid repeating units indicate the successful synthesis of the polymers. The decreased molecular weight upon incubation with 10 mM GSH also proves the redox sensitivity of the polymer.

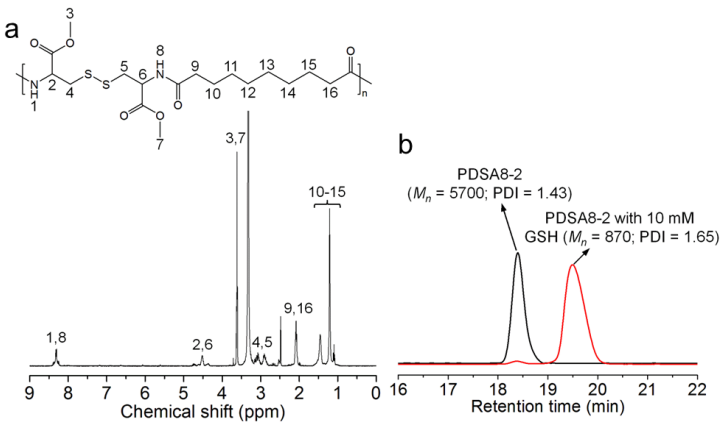

Figure 4. (a) ^{1}H-NMR spectrum of the Cys-PDSA8-2 in DMSO-*d*6; (b) GPC profile of Cys-PDSA8-2 incubated with 10 mM GSH for 4 h.

a	Cys-PDSA4	Cys-PDSA6	Cys-PDSA8-1	Cys-PDSA8-2	Cys-PDSA8-3	Cys-PDSA8-4
Size (nm)	155.7	134.5	118.9	102.9	99.4	93.4
EE%	29.7	35.1	46.3	55.9	79.4	88.2
ξ (mV)	-6.79	-8.08	-9.79	-11.21	-12.05	-20.01

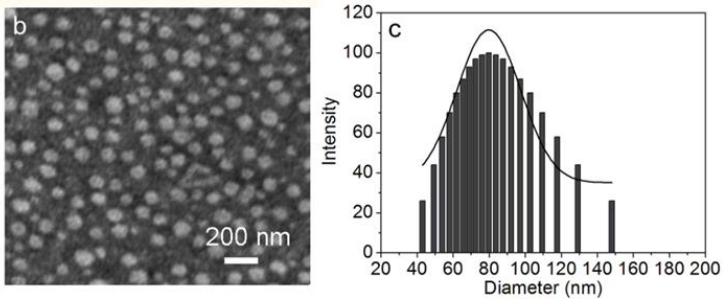

Figure 5. (a) Size, EE%, and zeta potential of Cys-PDSA NPs. (b, c) Morphology (b) and size distribution (c) of the siRNA loaded Cys-PDSA8-2 NPs.

We next studied the physiochemical properties of the NPs prepared from above polymers. Through mixing with lipid-PEG (DSPE-PEG) and cationic lipid-like compound (G0-C14), the polymers can self-assemble with siRNA into spherical NPs, with the differential particle size and siRNA encapsulation efficiency (EE%) depending on the aliphatic chain length of fatty diacid repeating unit and molecular weight of the polymers. With the increased aliphatic chain to improve the hydrophobicity of the polymers, the particle size decreases while the siRNA loading ability increases (Figure 5a). Figure 5b-c shows the spherical morphology

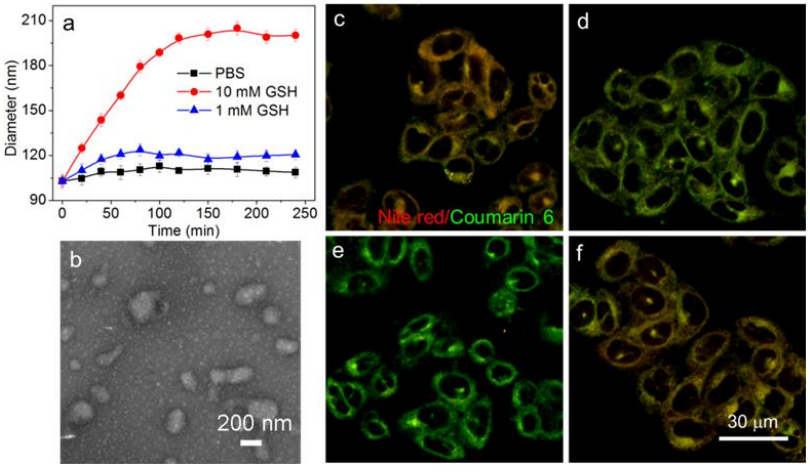

Figure 6. (a) Average size of siRNA loaded Cys-PDSA8-2 NPs incubated with GSH-containing PBS solution; (b) Morphology of the siRNA loaded Cys-PDSA8-2 NPs incubated in 10 mM GSH solution for 4 h; (c-f) Fluorescent images of HeLa cells incubated with the Nile red/coumarin 6 loaded Cys-PDSA8-2 NPs for 30 min (c); 1 h (d); 4 h (e), and NEM pre-treated HeLa cells incubated with the Nile red/coumarin 6 loaded Cys-PDSA8-2 NPs for 4 h.

and size distribution of the siRNA loaded NPs prepared from Cys-PDSA8-2. If incubating these NPs in GSH-containing aqueous solution, the degradation of the polymer induces the particle size increase (Figure 6a) and the morphology of NPs changes from spherical into irregular shape (Figure 6b). We further encapsulated Förster resonance energy transfer (FRET) pair consisting of coumarin 6 and Nile red into the NPs to evaluate the intracellular redox response. In this experiment, upon excitation of the donor dye (coumarin 6, excited at 400 nm), the emitted energy will be transferred to the acceptor dye (Nile red) due to its close proximity (< 10 nm), and thus red fluorescence can be detected. Upon destroying of the NPs by intracellular GSH, the FRET pair will be separated and thereby green fluorescence of the coumarin 6 can be restored, whereas the Nile red will stop fluorescing. Figures 6c-6f show the fluorescent images of HeLa cells incubated with Nile red/coumarin 6 loaded NPs. After 1 h, the red fluorescence resulting from the FRET decreased, whereas the green fluorescence of coumarin 6 increased. After 4 h, the cells show a dominant green color, and the red color is difficult to detect. If the cells were pretreated with 50 μM N-ethylmaleimide (NEM) for 1 h, an inhibitor that can react with thiols and reduce the effective concentration of intracellular GSH, the FRET effect persists after 4 h incubating with the NPs.

We also evaluated the silencing efficacy of the siRNA loaded NPs with Luc-HeLa cells. Figure 7a shows the expression of luciferase in HeLa cells treated with anti-luciferase siRNA loaded Cys-PDSA NPs. All these siRNA loaded NPs can knock down the luciferase expression, with the differential silencing efficacy depending on the composition of the NPs. Overall, the NPs composed of Cys-PDSA8 showed better gene silencing efficacy than the NPs made by other polymers. Moreover, among all the Cys-PDSA8 NPs, the NPs of the Cys-PDSA8-2 with a molecular weight of 5700 show the best gene silencing efficacy (>90% luciferase knockdown at 10 nM siRNA dose).

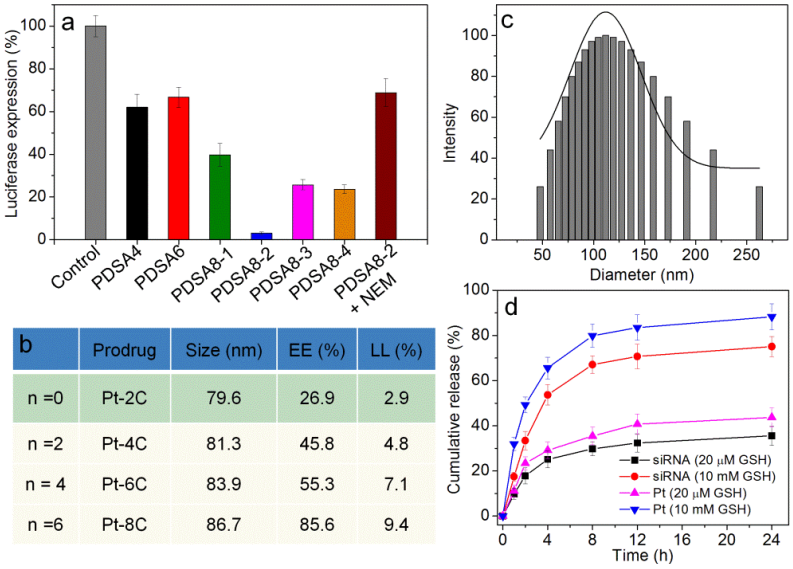

b	Prodrug	Size (nm)	EE (%)	LL (%)
n =0	Pt-2C	79.6	26.9	2.9
n =2	Pt-4C	81.3	45.8	4.8
n = 4	Pt-6C	83.9	55.3	7.1
n =6	Pt-8C	86.7	85.6	9.4

Figure 7. (a) Luciferase expression in HeLa cells incubated with the siRNA loaded Cys-PDSA8-2 NPs; (b) Size, EE%, and LL% of the cisplatin prodrug loaded Cys-PDSA8-2 NPs; (c) Size distribution of Pt-8C loaded Cys-PDSA8-2 NPs; (d) siRNA and cisplatin release from the siRNA/Pt-8C loaded Cys-PDSA8-2 NPs.

Current ongoing experiments include (1) the evaluation of lipid-PEG effect on luciferase gene silencing; (2) the testing of different cationic lipid or lipid-like materials on gene silencing; and (3) the use of the optimized parameters from lipid-PLGA hybrid NPs (e.g., choice of organic solvent in NP preparation, lipid-PEG, and cationic lipid) to the formulation of Cys-PDSA-based hybrid NPs.

(ii) Synthesis of cisplatin prodrugs (Farokhzad and Shi, BWH)

In this subtask, we have synthesized a series of cisplatin prodrugs with different hydrophobicity, and employed NMR to demonstrate the successful synthesis. Figure 7 shows the synthesis route of the various cisplatin prodrugs. The cisplatin was first oxidized into *cis,trans,cis*-$[PtCl_2(OH)_2(NH_3)_2]$, which was then attacked by various fatty acid anhydrides (*e.g.*, acetic anhydride (n=0), succinic anhydride (n=2), adipic anhydride (n=4), and sebacic anhydride

(n=6)). Figure 8 shows the NMR spectrum of one representative cisplatin prodrug synthesized using sebacic anhydride. The typical signals corresponding to the protons of sebacic tails demonstrate the successful synthesis.

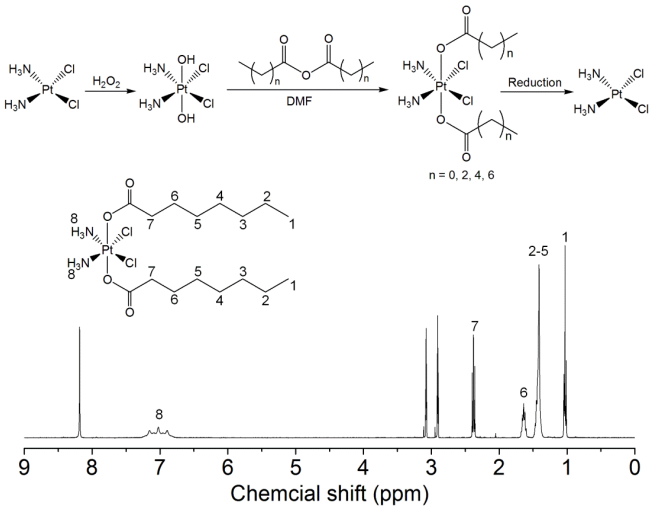

Figure 8. Synthesis route of the fatty acid conjugated cisplatin prodrugs, and ^{1}H-NMR spectrum of sebacic acid conjugated cisplatin prodrug in DMF-*d*7.

(iii) siRNA-Pt NP development (Farokhzad and Shi, BWH)

Based on the gene silencing result shown above, Cys-PDSA8-2 polymer was chosen to evaluate its ability to load cisplatin prodrugs. The prodrug loaded NPs were prepared via adding the mixture of Cys-PDSA8-2, DSPE-PEG and prodrug into water dropwise. Figure 7b shows the physiochemical properties of the prodrug loaded NPs. There is no significant difference in the size of the prodrug loaded NPs. However, with the increased aliphatic chain length to improve the hydrophobicity, the encapsulation efficiency (EE%) and loading level (LL%) of the resulting prodrugs increase. In particular, the EE% or LL% of the prodrug with sebacic tails (named as Pt-8C) can reach ~85.6% or 9.4%, respectively.

We chose Pt-8C and investigated the cisplatin and siRNA release of the Cys-PDSA8-2 NPs. Figure 7c shows the size distribution of the prodrug/siRNA loaded NPs. Compared with the siRNA loaded NPs, the co-delivery of prodrug and siRNA leads to a slight increase of the particle size from 102.9 nm (Figure 5a) to 113.7 nm. Figure 7d shows the cisplatin and siRNA release behaviors upon the addition of GSH. At a high GSH concentration (10 mM), more than 70% or 80% of loaded siRNA or cisplatin can be released within 24 h, while ~30-40% of loaded siRNA or drug was released at a low GSH concentration (20 μM).

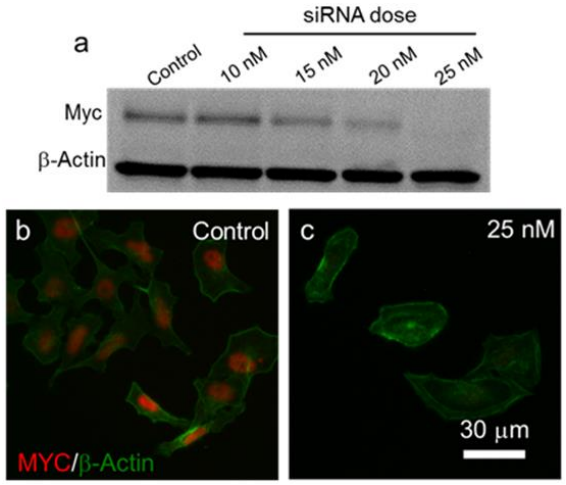

Figure 9. Western blot (a) and immunofluorescence (b, c) analysis of MYC expression in PC3 cells treated by MYC siRNA loaded Cys-PDSA8-2 NPs.

Major Task 2. In vitro evaluation and mechanism studies

(i) Cellular cytotoxicity of MYC siRNA-Pt NPs (Farokhzad and Shi, BWH)

In this subtask, we first used Cys-PDSA8-2 NPs to encapsulate MYC siRNA and evaluated the silencing of MYC in prostate cancer cell line (PC3 cells). Figure 9 shows the MYC expression in PC3 cells treated by MYC siRNA loaded NPs. Both western blot (Figure 9a) and immunofluorescence staining results (Figures 9b and 9c) demonstrate that the siRNA loaded NPs can efficiently knock down MYC expression in PC3 cells. Particularly, there is nearly no MYC expression at 25 nM siRNA dose.

We next studied the cytotoxicity of Pt-C8 loaded Cys-PDSA8-2 NPs against PC3 cells. Figure 10a shows the viability of PC3 cells incubated with the drug loaded NPs for 24 h. The half maximal inhibitory concentration (IC50) of cisplatin is around 18.4 mg/L while that of Pt-C8 loaded NPs showed comparable IC50 of ~ 22.7 mg/L. Based on the results of MYC silencing

and cytotoxicity assay, we then examined the influence of MYC siRNA or Pt-8C loaded NPs on the proliferation of PC3 cells (Figure 10b). Without any treatment, there is more than 12-fold increase in the cell number. With the silencing of MYC expression, there is ~ 4-fold increase at a siRNA dose of 35 nM. The Pt-8C NPs also significantly inhibited the cell proliferation and there is only ~ 2-fold increase in the cell number. Currently, we are working on the NP co-delivery of MYC siRNA and Pt-8C for the inhibition of PC3 cell growth.

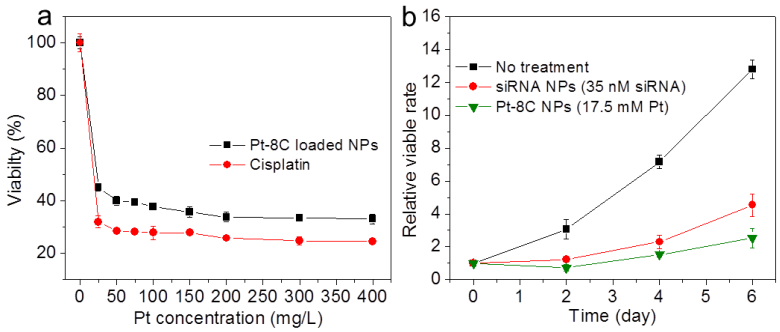

Figure 10. (a) Cytotoxicity of cisplatin and Pt-8C loaded Cys-PDSA8-2 NPs against PC3 cells; (b) Proliferation profile of PC3 cells treated with siRNA and Pt-8C NPs.

(ii) Mechanism study of the MYC role in Pt resistance (Farokhzad and Shi, BWH; De Marzo, JHU)

To investigate the MYC role in Pt resistance, we are now establishing Pt-resistant PC3 cells. The cells are being incubated in the culture medium containing cisplatin and the concentration of cisplatin is now increased gradually. After successfully obtaining Pt-resistant PC3 cells, we will then extensively investigate whether the MYC silencing can re-sensitize Pt-resistant PC3 cells to the treatment with cisplatin.

Major Task 3. In vivo test and optimization

(i) In vivo studies of select hybrid NPs (Farokhzad and Shi, BWH)

In this subtask, we first assessed the effect of lipid-PEG on PK of the hybrid siRNA NPs in normal mice after tail vein injection. Figure 11 shows that naked siRNA was rapidly cleared from systemic circulation within 30min, while siRNA NPs stayed longer in blood. Drastically different PK behaviors were observed among these NPs and between the neutral and anionic lipid-PEG categories. For the NPs coated with neutral lipid-PEGs, only the DSG-PEG NP exhibited a long circulation half-life ($t_{1/2}$) ~ 3.3h, with the other three NPs having $t_{1/2}$ < 20min (Figure 11a). The anionic lipid-PEG NPs showed longer circulation than the neutral counterparts (Figure 11b). DSPE-PEG NPs exhibited the most impressive circulation property with $t_{1/2}$ ~ 6h, and the area under the curve (AUC) is ~ 68-fold of that for naked siRNA. The trend found in the PK study for these lipid-PEG NPs analogously resembled that observed in the dissociation study (Figure 2d-e). We are now studying the effect of lipid-PEG on BioD and gene silencing in tumor tissues.

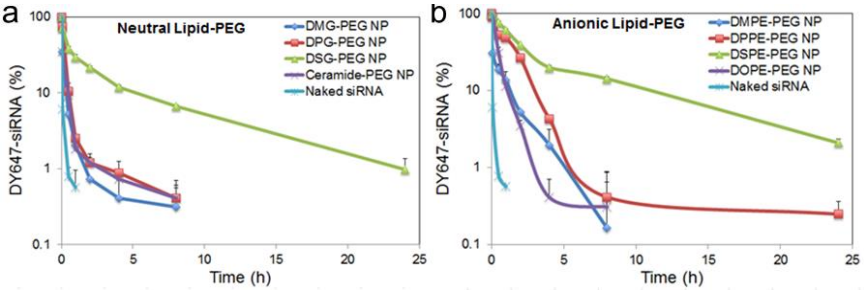

Figure 11. Effect of lipid-PEG on PK of the hybrid siRNA NPs.

(ii) In vivo evaluation of siRNA-Pt NPs (Bieberich, UMBC; De Marzo, JHU)

Establishment and maintenance of a Hoxb13-MYC$^{+|}$Hoxb13-Cre^{+}|Pten$^{fl/fl}$ colony: To generate the transgenic mice that develop lethal prostate cancers, we established breeding pairs characterized by the following genotypes*:* *Hoxb13-MYC$^{+/-}$|Hoxb13-Cre$^{+/-}$|Pten$^{fl/fl}$* X *Hoxb13-*

MYC$^{+/-}$|*Hoxb13-Cre*$^{+/-}$|*Pten*$^{fl/+}$. In offspring from crosses with these parental genotypes, we anticipated ~one in seven pups would be male and of the desired *Hoxb13-MYC*$^{+}$|*Hoxb13-Cre*$^{+}$|*Pten*$^{fl/fl}$ genotype (approximately one per litter, note that the *Hoxb13-MYC*$^{+}$ and *Hoxb13-Cre*$^{+}$ genotypes include both hemizygotes and homozygotes). Males with the *Hoxb13-MYC*$^{+}$|*Hoxb13-Cre*$^{+}$|*Pten*$^{fl/fl}$ are referred to as BMPC mice. Cohorts of BMPC mice are required to achieve the goals of Aims 2. Given the anticipated need for a cohort of 24 BMPC mice at 14 weeks of age, and 24 mice at 18 weeks of age to test the efficacy of MYC siRNA plus cisplatin-loaded NPs (RNAi-Pt NPs), and the need for ~10 BMPC males for RNAseq experiments, we immediately established 15 breeding pairs. Between October 2015 and October 2016, those breeding pairs generated 304 offspring that were screened using the services of Transnetyx, Inc. 63 BMPC males were identified. To date, three BMPC males have been used in experiments to determine the MYC signature, and the remainders are aging in the colony in anticipation of experiments to test the efficacy of RNAi-Pt NPs.

Establishment of cell lines derived from sites of metastasis of MYC-driven BMPC tumors: Although the BMPC model is a state-of-the-art preclinical model of MYC-driven human prostate cancer, it has now been in production for over eight years and is more than 30 generations from the original founder strains. Within the past year, we have observed an apparent decrease in the aggressiveness of the cancers that develop in these animals. Phenotypic drift in transgenic mouse models is a pervasive phenomenon and is thought to be the result of fixation of spontaneous mutations that arise randomly. To extend the utility of the BMPC model, and to provide an alternate platform in which RNAi-Pt NPs could be tested, we endeavored to generate BMPC cell lines from metastatic sites. To that end, two BMPC males with late stage disease (abdominal distention) were euthanized and an enlarged pelvic lymph node was removed from one, and an ~5 mm metastatic lesion in liver was removed from the other. After tissue disruption a using a Miltenyi gentleMACS™ dissociator, cells were plated in T75 flasks in Dulbecco's Modified Eagle's Medium (DMEM) plus 10% FBS in the presence of antibiotics. Upon confluence, cells were passaged as a bulk tumor cell population and

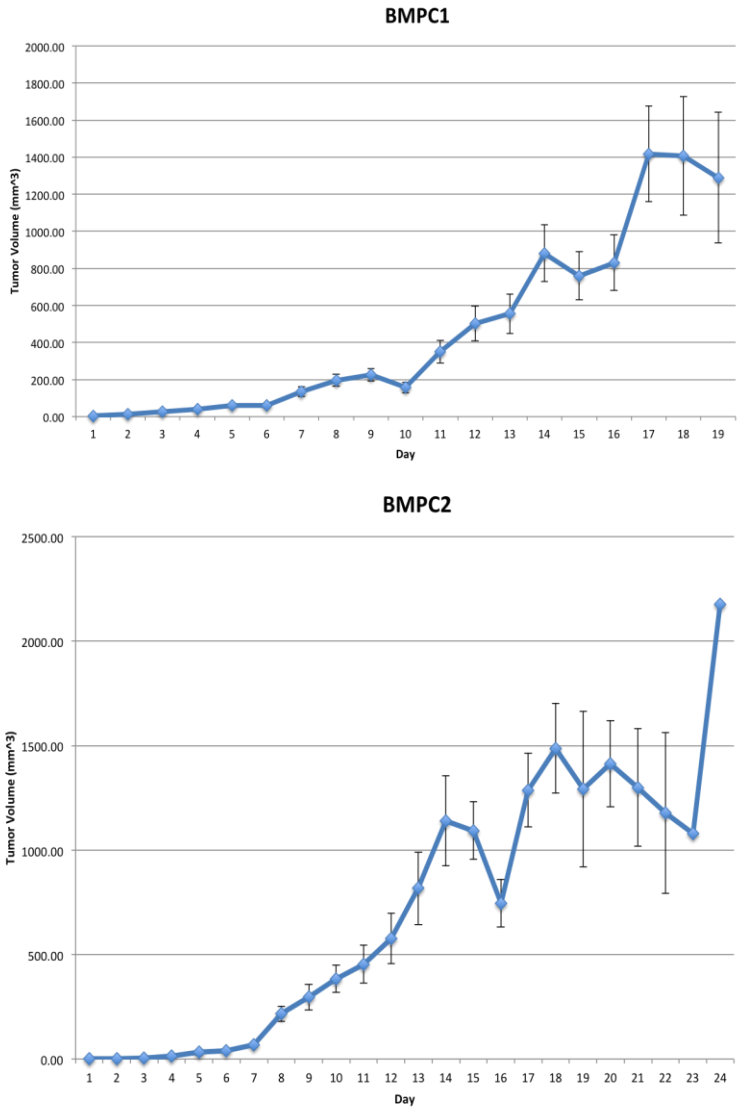

Figure 12. In vivo growth of BMPC1 and BMPC2 allograft tumors. Mean tumor volume (N=10) is shown +/- SE.

frozen at each passage. The bulk populations from both the liver and lymph node metastases continued robust growth beyond passage 10. In anticipation of using the cells in mouse allograft studies, both were sent to IXEDD BioResearch for testing for mouse and human pathogens. Both cells lines were determined to be pathogen free. Cells were then transferred from the Bieberich lab to co-P.I. Dr. Angelo De Marzo's laboratory for cloning. The cells were plated to single cell density in 100 mm culture dishes (Corning) in DMEM supplemented with 10% FBS until individual colonies were visualized. Cell media was then aspirated and discarded. Using sterile cloning cylinders (Corning) with silicone grease, individual colonies were isolated and harvested using 0.25% trypsin. Cells were transferred into a 6 well plate containing DMEM +10% FBS and subsequently passaged into T75 flasks. This process was carried out for cells derived from a lymph node metastasis and liver metastasis (described above). Five clones were isolated for each LN and liver metastasis. Each clone was screened for *Pten* loss and human MYC expression. LN clone #3 was renamed BMPC1 and liver clone #2 was renamed BMPC2. BMPC1 and BMPC2 were then returned to Dr. Bieberich's lab to investigate their ability to form allograft tumors.

Allograft tumor formation by BMPC1 and BMPC2 cells: To determine the growth characteristics of the BMPC1 and BMPC2 cell lines in vivo, 1×10^6 cells in DMEM were injected subcutaneously into the flank of athymic nude mice N=10). Within seven days, measurable allograft tumors arose in 19/20 and most had reached the maximum permissible tumor volume (1500 mm^3) within 24 days post-implantation (Figure 12). The high take rate and rapid growth of BMPC1 and BMPC2 allograft tumors positions them as an effective tool for initial determination of NP efficacy before transitioning to testing in the BMPC GEM model. The main advantage is that we can generate large perfectly age-matched cohorts of mice with similar tumor volumes. Although this approach was not in our original experimental strategy, we plan to continue to pursue this strategy to enable us to most efficiently achieve the goals of Aim 2. It is important to note that these experiments will not supplant, but will rather support, the GEM studies.

Phenotypic analysis of BMPC1 and BMPC2 cell lines: To determine how the phenotype of the BMPC cell lines compares with the BMPC mouse tumors, we performed IHC for a number of prostate markers and in situ hybridization with RNAscope for a number of mRNAs. The results to date show that BMPC1 and BMPC2 express Nkx3.1 (prostate specific) mRNA and protein, confirming their prostate origin. Both also express Hoxb13 mRNA and MYC mRNA and protein

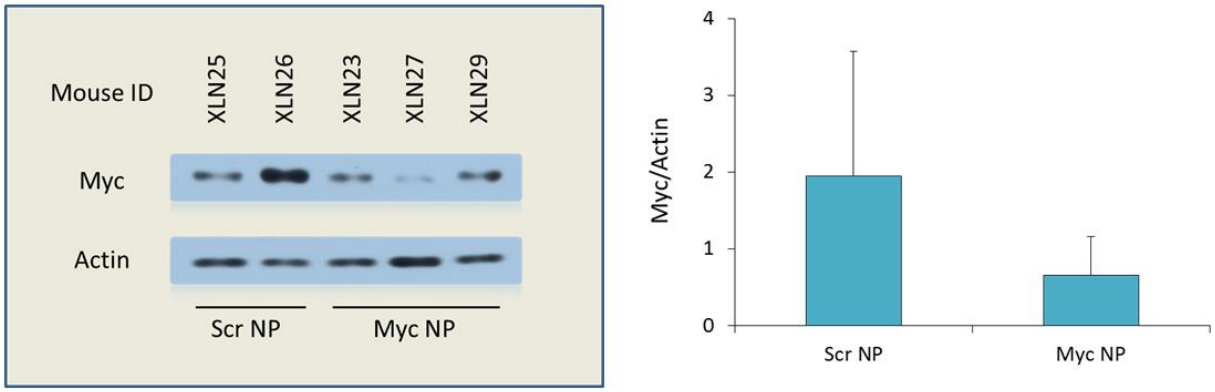

Figure 13. Effect MYC-siRNA NPs on MYC accumulation in BMPC allograft tumors in nude mice. Western blot (left panel) analysis of MYC expression in two tumors from mice injected with Cys-PDSA8-2 NPs loaded with a scrambled siRNA (SCR NP) and in three tumors from mice injected with Cys-PDSA8-2 NPs loaded with a MYC-targeting siRNA (MYC NP). Western blot films were scanned and MYC signal, normalized to actin signal, was quantified (right panel) based on pixel density. Mean signal (+/- SEM) is shown.

and are negative for Pten. Neither expresses basal cell markers. Interestingly, BMPC1 (and not BMPC2) expresses AR mRNA and also shows nuclear AR protein if the cells are treated with synthetic androgens.

MYC knockdown in BMPC allograft tumors: In anticipation of experiments wherein RNAi-Pt NPs will be injected into BMPC GEM mice, 1×10^6 BMPC1 cells were implanted into the flank of athymic nude mice. When BMPC1 tumors reached ~100 mm^3, 200 µl MYC-RNAi NPs was delivered via the tail vein at 24-hour intervals for three consecutive days. On day four, the mice were euthanized and tumors were resected. Where feasible, the tumors were divided in half for Western blot and histological quantification of MYC accumulation. Figure 13 shows that, while there was variability in MYC levels in the mice treated with the scrambled siRNA NPs, there was a reduction in MYC levels by western blot in the MYC NP treated mice. Similar results were seen in IHC with MYC levels (Figure 14), although quantification by blinded image analysis has not been completed yet.

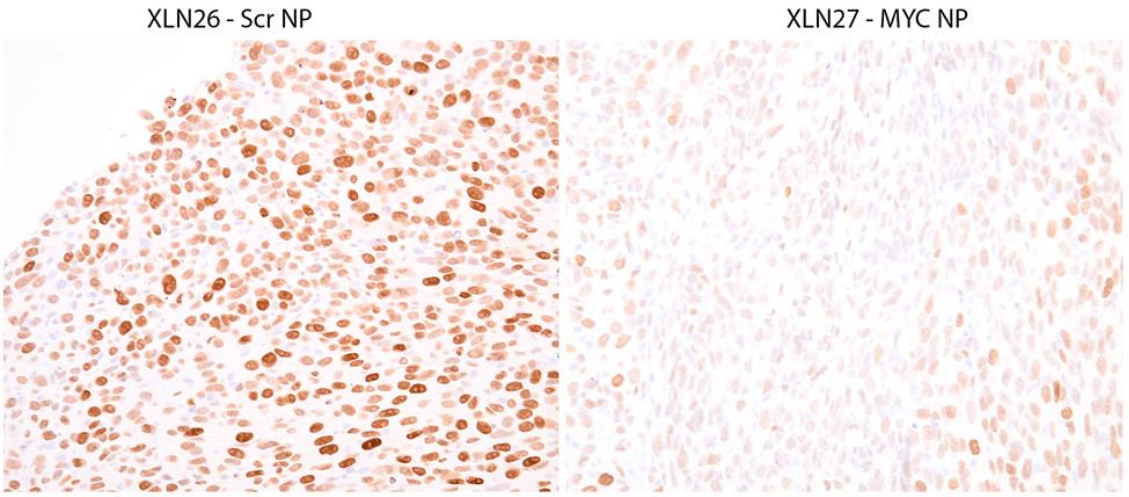

Figure 14. Effect of MYC-siRNA NPs on MYC levels in BMPC allograft tumors in nude mice. IHC carried out for MYC shows lower MYC signals in mice treated with MYC targeting NPs (Left). Original magnification × 200.

Major Task 4 (Subtask 2): MYC signature analysis in BMPC mice (Yegnasubramanian and De Marzo, JHU; Bieberich, UMBC)

In order to begin to determine whether our MYC signature from human prostate cancer cells lines is upregulated in primary tumors and metastatic lesion from the BMPC GEM mice, which we will lay the groundwork for detecting changes in such a signature after in vivo MYC-NP RNAi treatment, we performed RNAseq on 21 samples across all stages of disease including normal, PIN, invasive primary adenocarcinoma and metastatic disease and preliminary results are presented here.

RNAseq

RIN numbers for isolated RNA indicated that each sample contained excellent quality RNA. RNAseq was carried out using the Illumina TruSeq Stranded Total RNA sample prep using rRNA depletion without initial poly-A RNA selection. The sequencing runs were carried out using the HS2500 to 100x100 bp paired end reads in each sample. Table 1 shows the statistics from Sequencing runs. Illumina's CASAVA 1.8.2 was used to convert BCL to FASTQ files and

default parameters were used. RSEM was used to align to the mm10 mouse reference genome mouse genome and generate gene and isoform level expression measures. Tables of estimated expression were generated including TPM and FPKM measures. Tables of estimated isoform expression were also generated. Differential expression analysis of genes and isoforms was performed using EBSeq. Initial queries of differentially expressed genes were examined as a q/c measure and showed expected overall distributions in a number of genes queried. For example, Figure 15 shows that Ki67 [proliferation marker], fibrillarin/Fbl [nucleolar marker], and Ezh2 [polycomb group protein increased in all stages of prostate carcinogenesis] are increased in PIN and carcinoma [shown for PIN only], and basal cell markers [CK5 and CK15] were decreased in carcinoma compared to normal mouse prostate. Interestingly, *Hoxd13* (distinct from *Hoxb13*) has not previously been found to be downregulated in prostate cancer. However, we will be pursuing this further since a query of our separately supported human RNAseq data on prostate tumor and normal pairs confirms this marked down regulation (data not shown). These data from year 1 clearly show our ability to carry out RNAseq on isolated BMPC tumors and will be instrumental in subsequent years to derive a prostate cancer specific MYC-signature that can be utilized in our animal studies on BMPC GEM mice and the BMPC1 and BMPC2 cell line xenograft models after treatments with various NP formulations.

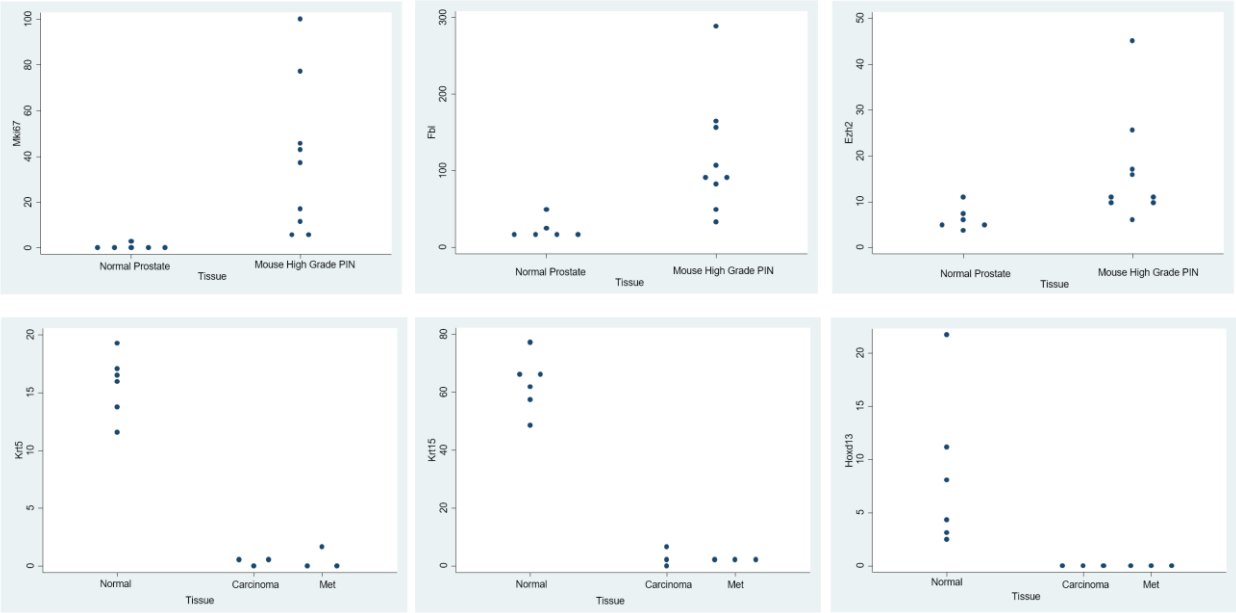

Figure 15. Select up and down regulated genes from RNAseq on mouse models of PIN and prostatic adenocarcinoma. The top panel shows 3 genes upregulated in all 3 types of PIN (3 samples each of *Hoxb13-MYC alone*, *Hoxb13-Cre*|*Pten*$^{Fl/Fl}$or BMPC = *Hoxb13-MYC*|*Hoxb13-Cre*|*Pten*$^{Fl/Fl}$). Normal prostate represents normal mouse prostate from FVB mice anterior and ventral lobes. The bottom panel shows select genes downregulated in invasive and metastatic BMPC mouse adenocarcinoma as compared to normal prostate. Note that to our knowledge *Hoxd13* has not previously been shown to be down regulated in prostate cancer.

Table 1. RNAseq number of reads and mapped reads from 21 samples.

Type	Lobe	tissue	organ	SampleName	Reads	rsem	%	rDNA (concordant)	%
fvb	ant	normal	prostate	MR01	123,449,603	35,551,704	28.80%	40,444,007	32.76%
fvb	ant	normal	prostate	MR02	216,625,111	58,503,612	27.01%	65,889,904	30.42%
fvb	ant	normal	prostate	MR03	133,206,810	43,792,624	32.88%	30,889,897	23.19%
fvb	vent	normal	prostate	MR04	128,970,701	60,796,855	47.14%	18,461,114	14.31%
fvb	vent	normal	prostate	MR05	108,498,770	45,025,166	41.50%	21,075,219	19.42%
fvb	vent	normal	prostate	MR06	48,922,872	23,093,159	47.20%	4,714,476	9.64%
b13myc	vent	pin	prostate	MR07	122,910,089	75,293,287	61.26%	11,267,209	9.17%
b13myc	vent	pin	prostate	MR08	54,961,729	29,130,414	53.00%	4,707,652	8.57%
b13myc	vent	pin	prostate	MR09	45,806,783	25,458,362	55.58%	3,945,769	8.61%
b13ptenff	ant	pin	prostate	MR10	104,429,690	59,198,731	56.69%	4,708,950	4.51%
b13ptenff	ant	pin	prostate	MR11	57,302,996	30,285,072	52.85%	2,020,457	3.53%
b13ptenff	ant	pin	prostate	MR12	73,630,333	33,177,175	45.06%	5,696,481	7.74%
bmpc	ant	pin	prostate	MR13	71,467,915	30,251,805	42.33%	7,627,980	10.67%
bmpc	ant	pin	prostate	MR14	119,437,996	50,041,758	41.90%	14,282,447	11.96%
bmpc	ant	pin	prostate	MR15	101,909,862	40,690,599	39.93%	14,163,841	13.90%
bmpc	unknown	priminv	prostate	MR16	90,034,022	45,364,575	50.39%	5,824,141	6.47%
bmpc	unknown	priminv	prostate	MR17	80,677,431	39,660,178	49.16%	-	0.00%
bmpc	unknown	priminv	prostate	MR18	54,378,964	17,280,260	31.78%	9,743,195	17.92%
bmpc	na	met	node	MR19	112,100,232	53,421,079	47.65%	7,024,719	6.27%
bmpc	na	met	node	MR20	51,216,830	23,129,591	45.16%	3,635,441	7.10%
bmpc	na	met	node	MR21	51,428,476	14,084,467	27.39%	12,030,509	23.39%

Bmpc= HoxB13-MYC/HoxB13-Cre/Pten$^{f/f}$ mice; B13ptenff= HoxB13Cre/Pten$^{f/f}$ mice; FVB=wild type control mice. Ant=anterior prostate. Vent=Ventral prostate. Na=not applicable. Pin= mouse prostatic intraepithelial neoplasia. Priminv= invasive primary adenocarcinoma. Met= metastatic adenocarcinoma.

- **What opportunities for training and professional development has the project provided?**

While the Brigham and Women's Hospital (BWH) does not have an institutional policy requiring individual development plans for postdoctoral fellows and graduate students, the hospital is very committed to training its students and fellows to meet their research and career goals. The hospital supports a centralized career development office, *Office for Research Careers of BWH Brigham Research Institute*, which offers seminars ranging from career development to responsible conduct of research to how to secure NIH and other external funding. The office also addresses the specific needs of postdoctoral fellows and faculty investigators in the research community at BWH, and supports BWH researchers across the academic continuum, by providing resources to support career and professional development, by encouraging professional responsibility, enhancing the training experience and fostering

effective mentoring. As a teaching affiliate of Harvard Medical School, BWH students and fellows have access to career development and support services offered by Harvard. Within my group, the postdoctoral fellows and students have routine meetings with me to discuss research project, skill and career development, and other needs they may have, and they present research work in the biweekly group meeting. The postdoctoral fellows and students are also encouraged and supported to attend local seminars, workshops, national conferences, and advanced education courses to present their research work, interact with colleagues, and enhance professional knowledge and skills, all of which will be helpful for their career development.

At Johns Hopkins there are a number of excellent opportunities for the professional development of our trainees related to this project. The pathology fellow is learning the histopathology of our prostate cancer mouse models and xenografts and also learning about IHC staining, in situ hybridization, automated whole slides scanning and digital image analysis. Also, one of our oncology fellows has been central in developing and characterizing the BMPC cell lines in which he has been involved in cell culture, cell cloning and phenotyping. We meet weekly with the pathology and oncology fellows in which we discuss their research and they present results. Also, we hold weekly and biweekly lab meeting with other collaborating labs, including Drs. Yegnasubramanian's lab. In terms of bioinformatics opportunities, Dr. Yegnasubramanian is mentoring a number of trainees who are working on the RNAseq data analysis and gene signatures. All trainees also have access to a number of lectures on cancer including our Fall Course on Cancer Biology given in the oncology department that meets twice per week and covers major topics related to cancer biology and treatment. Dr. Bieberich holds weekly meetings with his participating students and they are afforded a number of excellent opportunities. Drs. Bieberich, De Marzo and Yegnasubramanian hold periodic meetings to discuss the project and fellows and students often take part in these disucssions.

- **How were the results disseminated to communities of interest?**

Nothing to report.

- **What do you plan to do during the next reporting period to accomplish the goals?**

During the next reporting period, we will (i) further optimize and select the top NP formulation for siRNA delivery, by characterizing in vitro gene silencing, PK, BioD, in vivo toxicity, and gene silencing in tumor tissues; (ii) establish Pt-resistant PCa cells and investigate whether and how MYC silencing could re-sensitize Pt-resistant PCa cells to the treatment with cisplatin; (iii) characterize and optimize the RNAi-Pt NPs by testing different doses of cisplatin prodrugs and MYC siRNA in cytotoxicity studies with Pt-naïve and Pt-resistant PCa cells; and (iv) evaluate the therapeutic efficacy of RNAi-Pt NPs in PCa cell line-based xenograft and BMPC allograft tumor models.

At UMBC, we will continue to receive various NP formulations from Dr. Farokhzad's laboratory and continue to perform both xenograft and GEM model experiments with delivery of NPs for the studies outlined.

At Johns Hopkins, during the next reporting period we will continue to review all histopathology and perform immunohistochemistry and image analysis on the samples of NP treated animals performed in Dr. Bieberich's laboratory. With Dr. Yegnasubramanian's leadership we will be

continue to derive the MYC signatures and apply them to RNA isolated from the NP treated animal tissues to develop a pharmacodynamics marker panel to complement MYC IHC staining and western blotting as a readout of whether the NPs have hit their target (e.g., MYC).

4. IMPACT

- **What was the impact on the development of the principal discipline(s) of the project?**

During this reporting period, we have rationally designed and developed a new generation of lipid-polymer hybrid nanoparticles (NPs) with surface-tunable and redox-responsive properties. This unique NP platform is likely to make an impact on the field of RNA interference (RNAi), which holds significant potential for cancer therapy but requires effective and safe delivery to tumor tissues. Moreover, we have established cell lines derived from sites of metastasis of MYC-driven transgenic mice with prostate cancer. The allograft tumor models formed by these new prostate cancer cell lines could provide a robust animal platform for the evaluation and screening of drugs and therapeutic NPs. We have also carried out RNAseq experiments on the GEM models that will lay the groundwork for deriving our MYC signature that will be used as a pharmacodynamics marker in subsequent studies.

- **What was the impact on other disciplines?**

Nothing to report.

- **What was the impact on technology transfer?**

Nothing to report.

- **What was the impact on society beyond science and technology?**

Nothing to report.

5. CHANGES/PROBLEMS

- **Changes in approach and reasons for change**

In this reporting period, we have developed redox-responsive polymers and established cell lines derived from sites of metastasis of MYC-driven BMPC tumors, both of which were not in the original research plan. The reason to replace the PLGA polymer as used in the hybrid NP's core with the redox-responsive polymers is to further improve siRNA delivery to cancer cells. The high intracellular redox levels (e.g., glutathione) in cancer cells provide a natural stimulus for triggered cytosolic siRNA release. The reason to establish BMPC cell lines is to extend the utility of the BMPC GEM model, and to provide an alternate platform in which RNAi-Pt NPs could be tested effectively. This strategy will not supplant, but rather support the GEM studies in Aim 2. However, please note that there are no significant changes in objectives of this proposal.

- **Actual or anticipated problems or delays and actions or plans to resolve them**

Nothing to report.

- **Changes that had a significant impact on expenditures**

Nothing to report.

- **Significant changes in use or care of human subjects, vertebrate animals, biohazards, and/or select agents**

Nothing to report.

- **Significant changes in use or care of human subjects**

Nothing to report.

- **Significant changes in use or care of vertebrate animals**

Nothing to report.

- **Significant changes in use of biohazards and/or select agents**

Nothing to report.

6. PRODUCTS

- **Publications, conference papers, and presentations**

Journal publications:

1. Shi J, Kantoff PW, Wooster R, Farokhzad OC. Cancer Nanomedicine: Progress, Challenges and Opportunities. **Nat Rev Cancer** 2016; In press. (Acknowledgement of federal support: yes)
2. Xu X, Wu J, Liu YL, Zhao L, Zhu X, Bhasin S, Li Q, Shi J, Farokhzad OC. Ultra pH-Responsive and Tumor-Penetrating Nanoplatform for Targeted siRNA Delivery with Robust Anti-Cancer Efficacy. **Angew Chem Int Ed** 2016; 55(25):7091-4. (Acknowledgement of federal support: yes)

- **Website(s) or other Internet site(s)**

Nothing to report.

- **Technologies or techniques**

Nothing to report.

- **Inventions, patent applications, and/or licenses**

Stimuli-Responsive Nanoparticles for Biomedical Applications; Inventors: Xiaoding Xu, Jinjun Shi, Omid C. Farokhzad; US Provisional No. 62/317,033.

- **Other Products**

Nothing to report.

7. PARTICIPANTS & OTHER COLLABORATING ORGANIZATIONS

- **What individuals have worked on the project?**

BWH

Name:	*Omid C. Farokhzad*
Project Role:	*Initiating PI*
Researcher Identifier (e.g. ORCID ID):	
Nearest person month worked:	*0.6*
Contribution to Project:	*Dr. Farokhzad oversees the whole project.*
Funding Support:	

Name:	*Jinjun Shi*
Project Role:	*Co-investigator*
Researcher Identifier (e.g. ORCID ID):	
Nearest person month worked:	*1.2*
Contribution to Project:	*Dr. Shi has supervised the design and development of the hybrid siRNA NPs.*
Funding Support:	

Name:	*Xiaoding Xu*
Project Role:	*Postdoctoral Fellow*
Researcher Identifier (e.g. ORCID ID):	
Nearest person month worked:	*12*
Contribution to Project:	*Dr. Xu has lead the siRNA NP development and characterization, polymer synthesis, Pt prodrug synthesis, and in vitro/in vivo testing*
Funding Support:	

Name:	*Amanda Victorious*
Project Role:	*Undergraduate Student*
Researcher Identifier (e.g. ORCID ID):	*Ms. Victorious helped Dr. Xu with NP preparation and characterization, and in vitro testing*
Nearest person month worked:	*8*
Contribution to Project:	
Funding Support:	*Prostate Cancer Foundation*

JHU

Name:	*Angelo De Marzo*
Project Role:	*Partnering PI*
Researcher Identifier (e.g. ORCID ID):	
Nearest person month worked:	*0.6*
Contribution to Project:	*Dr. De Marzo oversees all experiments at JHU for pathology and sequencing of NP-treated tumor tissues.*

Funding Support:	
Name:	*Srinivasan Yegnasubramanian*
Project Role:	*Co-investigator*
Researcher Identifier (e.g. ORCID ID):	
Nearest person month worked:	*0.6*
Contribution to Project:	*Dr. Yegnasubramanian has supervised the sequencing experiments.*
Funding Support:	

Name:	*Jessica Hicks*
Project Role:	*Technician*
Researcher Identifier (e.g. ORCID ID):	
Nearest person month worked:	*0.6*
Contribution to Project:	*Mrs. Hicks performed IHC assays on the NP treated tissues*
Funding Support:	

UMBC

Name:	*Charles Bieberich*
Project Role:	*Partnering PI*
Researcher Identifier (e.g. ORCID ID):	
Nearest person month worked:	*2*
Contribution to Project:	*Dr. Bieberich oversees all experiments at UMBC to test nanotherapies in BPMC GEM models and in allograft-bearing mice.*
Funding Support:	*Prostate Cancer Foundation*

Name:	*Shuaishuai Liu*
Project Role:	*Graduate student*
Researcher Identifier (e.g. ORCID ID):	
Nearest person month worked:	*6*
Contribution to Project:	*Injection of BMPC cells to generate allograft tumors; injection of RNAi NPs into BMPC GEM and BMPC allograft mice; Western blot analysis of MYC expression*
Funding Support:	

Name:	*Apurv Rege*
Project Role:	*Graduate student*
Researcher Identifier (e.g. ORCID ID):	
Nearest person month worked:	*12*
Contribution to Project:	*Maintenance of BMPC colony; Genotypic analysis of BMPC mice*
Funding Support:	*Prostate Cancer Foundation*

- **Has there been a change in the active other support of the PD/PI(s) or senior/key personnel since the last reporting period?**

Nothing to report.

- **What other organizations were involved as partners?**

We have two partnering organizations in this project.

Partnering PI: Angelo M. De Marzo; Co-I: Srinivasan Yegnasubramanian
Organization Name: The Johns Hopkins University
Organization Location: School of Medicine, 733 N Broadway Baltimore, MD 21205
Partner's Contribution: Collaboration

Partnering PI: Charles J. Bieberich
Organization Name: University of Maryland, Baltimore County
Organization Location: Department of Biological Sciences, 1000 Hilltop Rd, Baltimore, MD 21250
Partner's Contribution: Collaboration

8. SPECIAL REPORTING REQUIREMENTS

➢ COLLABORATIVE AWARDS

This collaborative award is led by Initiating PI (Dr. Farokhzad) and Partnering PIs (Drs. De Marzo and Bieberich). We prepared the report together, and the tasks are clearly marked with the responsible PI and research site as shown in **3. ACCOMPLISHMENTS**.

➢ QUAD CHARTS

Nothing to report.

9. APPENDICES

Nothing to report.